

PHASE-FREQUENCY CHARACTERISTICS OF THE LONGITUDINAL AND TRANSVERSE VIBRATIONS OF PLANAR PIEZOCERAMIC TRANSFORMERS

V. L. Karlash

Experimental data on longitudinal and transverse vibrations of thin lamellar piezotransformer are analyzed. It is established that the voltage drops and instantaneous powers are very sensitive to the loading conditions, while the admittances, impedances, and phase shifts do not depend on them. If the current is set constant, the instantaneous power decreases as the resonance is approached and increases as the antiresonance is approached. If the voltage is set constant, the instantaneous power increases as the resonance is approached and decreases as the antiresonance is approached

Keywords: piezoceramic transformer, instantaneous power, admittance, impedance, phase shift, efficiency

Introduction. Planar piezoelectric voltage and current transformers [3, 6, 12, 15, 36] are successfully applied in various fields of engineering, such as in sources of secondary power sources (SPS) where constant voltages are converted from one (low) level to another (high) level [3]. As components of automatic frequency–amplitude–phase-controlled generators in such sources, piezoelectric transformers maintain constant output voltage. The main parameters of piezoelectric transformers are transformation ratios, working frequencies, output voltage and current, efficiency, power, strength, life. The last two parameters are strongly dependent deformation behavior and stress state. Designs of piezoelectric transformers for special operating conditions are described in [11, 12, 36]. The cylindrical panel described in [25] is a kind of three-layer transformer.

Formulas for transformation ratios were derived by, mainly, the equivalent-circuit method and are valid only for the first resonance [3, 7, 26]. In [4, 9, 15–20], an analytical method for studying the stress state and frequency properties of a Rosen-type piezoelectric transformer was developed, refined formulas for the voltage transformation ratio of an idling transformer were derived, the effect of the electroelastic inhomogeneity of the sections on the frequency properties was evaluated, and the stress state of planar piezoelectric transformers was studied experimentally by the piezotransformer transducer method for several vibration modes.

After the development of the advanced method for determining amplitudes and phases from successive measurement of the voltage drops across the piezoelectric element and the pull-up resistor [5, 10, 21, 23, 24, 31], it became possible to study the behavior of the phase, admittance, and power of a piezoelectric transformer over a wide frequency range.

Here we will analyze experimental results on the amplitude–frequency and phase–frequency responses (AFR and PFR) of a planar piezoelectric transformer in the frequency range of longitudinal and transverse vibrations. The phase and power characteristics are addressed for the first time.

1. Transformation Ratio and Input Admittance of a Planar Piezoelectric Transformer. Models of a planar piezoelectric transformer were detailed in [4, 9, 26, etc.]. It consists of input and output sections. The input section has length l_1 , is covered by thin electrodes, and polarized across the thickness to saturation. The output section has length l_2 , is covered by electrode coating on the end ($y = l_2$), and is polarized along the length to saturation. The sections have different electrophysical parameters. The thickness $2h$ and width $2b$ do not usually vary along the length. The lengths l_1 and l_2 are usually equal.

A variable voltage V_1 generated by an external generator is applied to the input (excitation) section, inducing electromechanical vibrations and electric current I_1 . Due to the vibrations and deformation of the plate, the induced piezocharge Q_2 of the output (generating) section generates voltage V_2 across and current I_2 in the output electrode.

Assume that the mechanical stresses at the ends of the plate are zero, and the stresses and displacements are continuous at the interface between the sections:

$$\sigma_y|_{y=-l_1} = \sigma_y|_{y=l_2} = 0, \quad \sigma_y(-0) = \sigma_y(+0), \quad u_y(-0) = u_y(+0). \quad (1)$$

The notation is the same as in [4, 10, 15–23]. The electrodes in the excitation section are equipotential; therefore,

$$\left. \frac{\partial E_x}{\partial y} \right|_{y<0} = \left. \frac{\partial E_x}{\partial z} \right|_{y<0} = 0, \quad (2)$$

and the electric-flux density in the generating section is assumed constant [27]:

$$\left. \frac{\partial D_x}{\partial y} \right|_{y>0} = \left. \frac{\partial D_y}{\partial y} \right|_{y>0} = 0. \quad (3)$$

The problem of the longitudinal vibrations of such an inhomogeneous plate was solved in [4, 9, 18] where expressions for the displacements and stresses in the sections and for the input current and output voltage were derived:

$$U_{y1} = \frac{(d_{31}E_{x1}\Delta - Ak_1 \sin k_1 l_1) \sin k_1 y + Ak_1 \cos k_1 l_1 \cos k_1 y}{k_1 \Delta \cos k_1 l_1}, \quad (4)$$

$$\sigma_{y1} = \frac{d_{31}E_{x1}\Delta \cos k_1 y - Ak_1 \sin k_1 l_1 \cos k_1 y}{\Delta s_{11}^E \cos k_1 l_1} - \frac{Ak_1 \sin k_1 y + d_{31}E_{x1}\Delta}{s_{11}^E \Delta}, \quad (5)$$

$$U_{y2} = \frac{(g_{33}D_{y2}\Delta + Ak_2 \sin k_2 l_2) \sin k_2 y + Ak_2 \cos k_2 l_2 \cos k_2 y}{k_2 \Delta \cos k_2 l_2}, \quad (6)$$

$$\sigma_{y2} = \frac{g_{33}D_{y2}\Delta \cos k_2 y + Ak_2 \sin k_2 l_2 \cos k_2 y}{s_{33}^D \Delta \cos k_2 l_2} - \frac{Ak_2 \sin k_2 y + g_{33}D_{y2}\Delta}{s_{33}^D \Delta}, \quad (7)$$

$$I_1 = j\omega \int_{s1} D_{x1} ds = -j\omega C_{01}^T V_1 \left(1 - k_{31}^2 + \frac{k_{31}^2 \tan k_1 l_1}{k_1 l_1} \right) + j\omega \frac{C_{01}^T V_1 k_{31}^2 s_{33}^D \cos k_2 l_2}{l_1 \Delta \cos k_1 l_1} (1 - \cos k_1 l_1)^2 - j\omega \frac{2bd_{31}d_{33}D_{y2}}{\varepsilon_{33}^T \Delta} (1 - \cos k_1 l_1)(1 - \cos k_2 l_2), \quad (8)$$

$$V_2 = -\int_0^{l2} E_{y2} dy = -\beta_{33}^T D_{y2} l_2 \left(1 + k_D^2 - \frac{k_D^2 \tan \gamma x}{\gamma x} \right) + \frac{g_{33}^2 s_{11}^E D_{y2} \alpha_2^2 \cos x}{s_{33}^D \Delta \cos \gamma x} + \frac{g_{33} d_{31} V_1 \alpha_1 \alpha_2}{2h\Delta}, \quad (9)$$

where

$$A = s_{33}^D d_{31} E_{x1} \cos k_2 l_2 (1 - \cos k_1 l_1) - s_{11}^E g_{33} D_{y2} \cos k_1 l_1 (1 - \cos k_2 l_2),$$

$$\Delta = s_{11}^E k_2 \cos k_1 l_1 \sin k_2 l_2 + s_{33}^D k_1 \sin k_1 l_1 \cos k_2 l_2 \quad (k_1^2 = \rho \omega^2 s_{11}^E, \quad k_2^2 = \rho \omega^2 s_{33}^D), \quad (10)$$

$$C_{01}^T = \frac{2bl_1 \varepsilon_{33}^T}{2h}, \quad C_{01}^S = (1 - k_{31}^2) C_{01}^T, \quad k_{31}^2 = \frac{d_{31}^2}{s_{11}^E \varepsilon_{33}^T}, \quad V_1 = -2E_{x1} h, \quad (11)$$

$$k_{33}^2 = \frac{d_{33}^2}{s_{33}^E \varepsilon_{33}^T}, \quad k_D^2 = \frac{g_{33}^2}{s_{33}^D \beta_{33}^T}, \quad g_{33} = \frac{d_{33}}{\varepsilon_{33}^T}, \quad \beta_{33}^T = \frac{1}{\varepsilon_{33}^T} \quad (12)$$

$$(x = x_1 = k_1 l_1, \quad x_2 = k_2 l_2, \quad x_2 / x_1 = \gamma, \quad \alpha_1 = 1 - \cos x, \quad \alpha_2 = 1 - \cos \gamma x, \quad \delta = l_2 / l_1).$$

The electric-flux density in the generating section of an idling piezoceramic transformer is assume equal to zero [9]; then the expression for V_2 becomes simpler:

$$V_2 = \frac{g_{33} d_{31} V_1 \alpha_1 \alpha_2}{2h\Delta}. \quad (13)$$

The ratio $K_{12} = V_2 / V_1$ is the transformation ratio of an idling piezoelectric transformer:

$$K_{12} = \frac{g_{33} d_{31} \alpha_1 \alpha_2}{2h\Delta}. \quad (14)$$

This ratio increases with increase in the piezoelectric moduli of both sections and the ratio $\alpha_1 \alpha_2 / \Delta$ and with decrease in the thickness of the plate. The denominator of this fraction vanishes at resonant frequencies, so that K_{12} tends to infinity. This can be avoided by introducing mechanical losses as a dimensionless complex frequency x [8, 13, 26]:

$$x = x' - jx'' = x' \left(1 - \frac{j}{2Q_m} \right). \quad (15)$$

Taking into account this circumstance, a refined formula for the magnitude of the transformation ratio at a resonance was derived in [4, 10, 20]:

$$|K_{12}| = \frac{l_1}{2h} \frac{d_{33} |d_{31}|}{s_{11}^E \varepsilon_{33}^T} \frac{2Q_m}{\delta x' \gamma x'} \frac{(1 - \cos x')(1 - \cos \gamma x')}{(1 + \gamma^2 \delta) \sin x' \sin \gamma x' - \gamma(1 + \delta) \cos x' \cos \gamma x'}. \quad (16)$$

The ratio of input current to input voltage is input conductivity (input admittance), and the ratio of output voltage to output current is output impedance:

$$Y_{in} = I_1 / V_1, \quad Z = V_2 / I_2. \quad (17)$$

2. Experimental Procedure and Results. In the experiments, we used an advanced Mason circuit detailed in [5, 10, 21, 24, 31].

The piezoelectric element in the classical Mason circuit is the link between the pull-up resistor and the ultrasonic generator [2, 9, 21]. One terminal of the pull-up resistor is connected to the common (“grounded”). As the generator is tuned, the voltage across the pull-up resistor increases at the resonant frequencies and decreases at the antiresonant frequencies severalfold (compared with the capacitive component). The frequencies at which the voltage across the pull-up resistor is maximum correspond to the maximum admittance of the piezoelectric element and are usually considered resonant ones. The frequencies corresponding to the minimum admittance or the minimum voltage across the pull-up resistor are considered antiresonant ones. It is possible to “inverse” the measuring portion of the Mason circuit by connecting it to the generator so as to “ground” one of the terminals of the piezoelectric element. This would make the direct measurement of the voltage across the piezoelectric element possible. However, the voltage across the pull-up resistor would have to be measured indirectly.

Combining the “direct” and “inverse” measuring portions of the Mason circuit, as done in [5, 10], we can raise the accuracy of determining the admittance in a frequency range and exclude the influence of phase shifts. To this end, it is necessary to connect a switch into the measuring circuit to alternately “ground” one terminal of the pull-up resistor or one terminal of the piezoelectric element. The voltage U_R across the pull-up resistor is proportional to the current I_{pe} in the piezoelectric element, and the voltage U_{pe} across the piezoelectric element can be measured at the same frequency by the same voltmeter, so that the following simple formula can be used to determine the admittance Y_{pe} of the piezoelectric element:

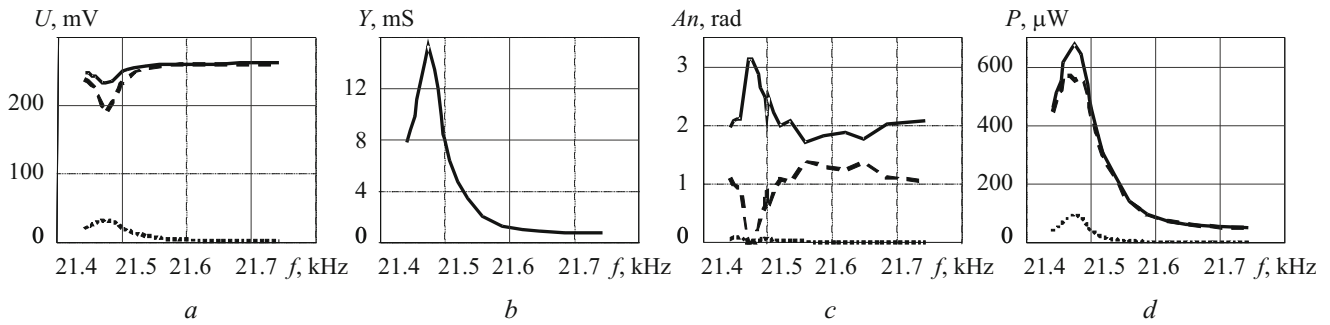


Fig. 1

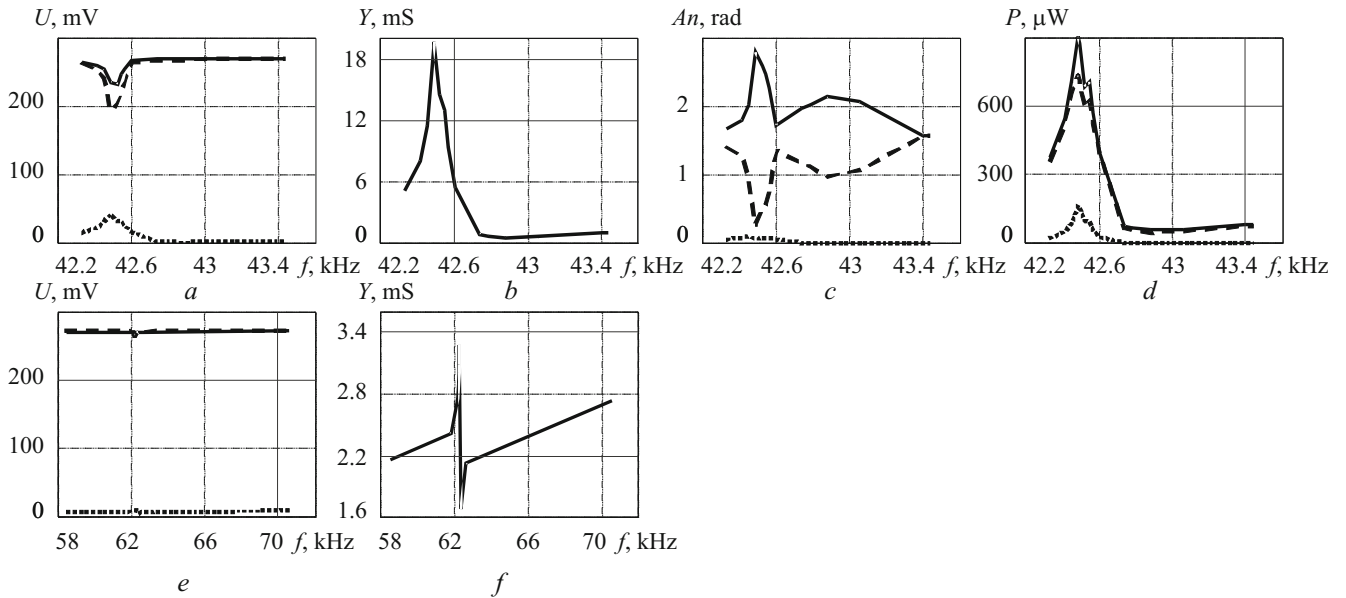


Fig. 2

$$Y_{pe} = \frac{I_{pe}}{U_{pe}} = \frac{U_R}{RU_{pe}}. \quad (18)$$

We studied a planar $80 \times 18 \times 2$ mm Rosen-type piezoelectric transformer made of PKD piezoceramics [4, 20] in the frequency range 20–110 kHz, which covered both longitudinal and transverse vibrations. Sequentially measured voltage U_R across the pull-up resistor, the voltage U_{pe} across the specimen, and the input voltage U_{in} of the measurement circuit (output of the generator or voltage divider) were used to compute the components of input conductivity, input impedance, phase angles or instantaneous power P , and its active P_a and reactive P_{re} components at the frequencies of measurement. The following formulas were used:

$$\cos \alpha = \frac{U_{pe}^2 + U_R^2 - U_{in}^2}{2U_{pe}U_R}, \quad \cos \beta = \frac{U_{in}^2 + U_R^2 - U_{pe}^2}{2U_{in}U_R}, \quad \cos \gamma = \frac{U_{in}^2 + U_{pe}^2 - U_R^2}{2U_{in}U_{pe}}, \quad (19)$$

$$P = V_1 I_1, \quad P_a = V_1 I_1 \cos j, \quad P_{re} = V_1 I_1 \sin j$$

$$(w_1 = \text{Re}(Y) / \text{Im}(Y), j = \text{acot}(w_1)). \quad (20)$$

In the frequency range 20–110 kHz, there are seven modes of different intensity, from the first longitudinal L_1 (first resonance) to the intensive transverse T_1 (fifth resonance).

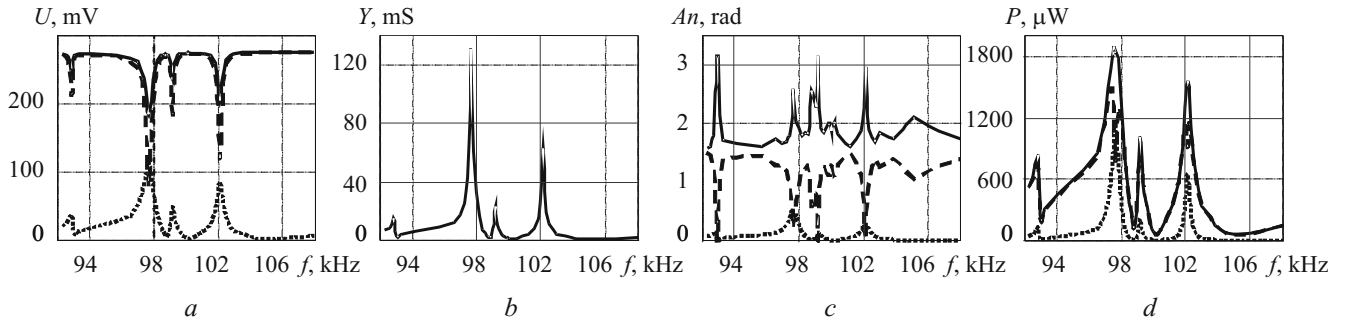


Fig. 3

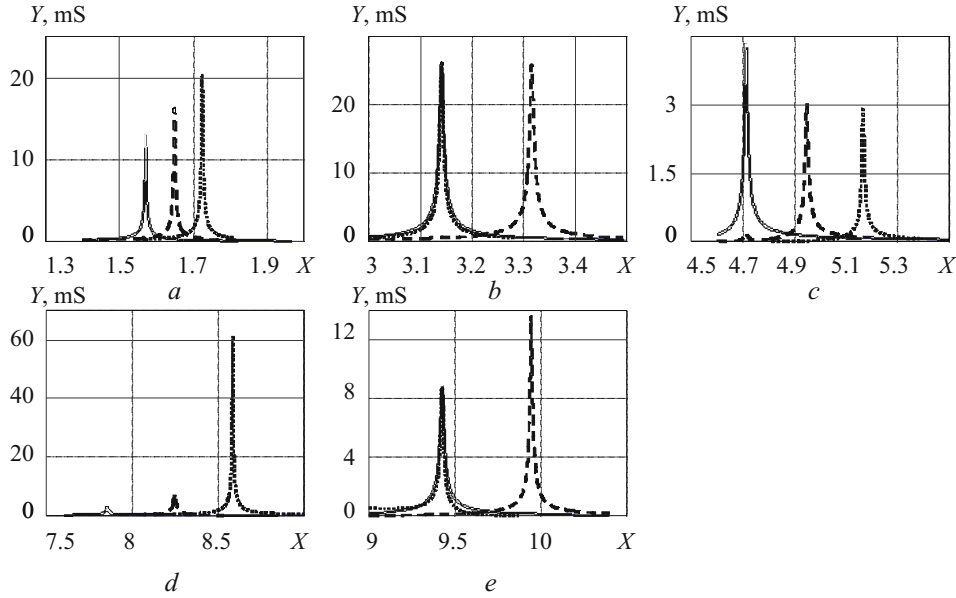


Fig. 4

Figure 1 illustrates the frequency dependence of voltage (Fig. 1a), input conductivity (Fig. 1b), phase shifts (Fig. 1c), and instantaneous power (Fig. 1d) at the first resonance.

Figure 2 illustrates similar curves at the second resonance, and the frequency dependence of voltage (Fig. 2e) and input conductivity (Fig. 2f) at the third longitudinal resonance.

Figure 3 represents the frequency range 92–108 kHz that includes the four resonances accompanying the intensive (transverse) fifth mode. The voltages U_{in} , U_{pe} , and U_R are shown by solid, dotted, and dashed lines, respectively. The angles α , β , γ and powers P_{in} , P_{pe} , P_r are shown by similar lines. The power P_{in} is consumed from the generator, the power P_{pe} is generated by the piezoelectric element during measurements, and the power P_r is generated by the pull-up resistor. The angle α is formed by the sides U_R and U_{pe} of the triangle. It characterizes the phase shift between the current through and the voltage drop across the specimen. The angle β is formed by the sides U_{in} and U_R and characterizes the phase shift between the output voltage and the consumed current. The angle γ is formed by the sides U_{in} and U_{pe} , i.e., it is the phase shift between the output voltage of the generator and the voltage drop across the piezoelectric transformer.

Figure 4 compares the experimental and calculated (by formula (17) with (8) and (15)) values of input admittance in the following dimensional frequency ranges: 1.4–2.0 (at the first longitudinal resonance, Fig. 4a); 3–3.5 (at the second longitudinal resonance, Fig. 4b); 4.6–5.5 (at the third resonance, Fig. 4c); 7.5–9 (at the fifth resonance, Fig. 4d); 9–11 (at the sixth resonance, Fig. 4e). According to [10, 17], the fourth longitudinal resonance at the frequency $x=2\pi$ is not excited in a Rosen-type piezoelectric transformer; therefore, there are no experimental and theoretical data on it. The solid, dashed, and dotted lines correspond to $\gamma = 1, 0.9, 0.8$. The factor ωC_0 was replaced by the expression

$$\omega C_0 = (2\pi f x C_0) / f_0 = ax, \quad (21)$$

where f is the frequency of loading; x is the dimensionless frequency; f_0 is the frequency of maximum input admittance at the first mode. The factor a in formula (21) was calculated using the following real parameters of the transformer: $C_0 = 5300$ pF (capacitance of the input section), $\tan d_1 = 0.0047$ (loss tangent of the input section), $C = 12.5$ pF (capacitance of the output section), $\tan d_2 = 0.005$ (loss tangent of the output section), $R = 11.2 \Omega$ (the pull-up resistor in the measurement circuit), $Q = 450$ (Q-factor determined from the frequency-dependence of the transformation ratio in the first vibration mode), so that $a = 0.455$ mS. The squared transverse EMCC $k_{31}^2 = 0.12$.

3. Analysis of the Results. The frequency dependences of voltages, admittances, phase shifts, and instantaneous powers for seven vibration modes of a $80 \times 18 \times 2$ mm planar Rosen-type piezoelectric transformer were established experimentally. An advanced Mason circuit with a switch and at a load of 11.2Ω was used. The curves were plotted for the first three resonances and frequency range 92–108 kHz. If the pull-up resistor is 11.2Ω , the near resonance domains were detected well (can be seen in the figures). The antiresonances and domains around them are smoothed out through by shunting the parallel resonance by a low pull-up resistor. The effect of the pull-up resistor on the results should be analyzed separately.

The admittances of the transverse resonances are almost an order of magnitude higher than those of the longitudinal resonances. The intensities of the first two modes are almost equal. The phase dependences for the strong and weak modes are similar.

The figures demonstrate the strong influence of the factor γ , which characterizes the difference of the compliances of the input and output sections of the piezoelectric transformer. This influence is different for even and odd modes. Unlike a transversely polarized rod, which does not have even modes, modes with frequencies multiple of 2π are not excited in a piezoelectric transformer [4, 9, 18–20].

Conclusions. The analysis of the experimental data on longitudinal and transverse vibrations of a thin planar piezoelectric transformer has revealed the following. Voltages and instantaneous power are rather sensitive to the electric loading conditions. Admittance, impedance, and phase shifts do not depend on them. If the current is set constant, the instantaneous power decreases as the resonance is approached and increases as the antiresonance is approached. If the voltage is set constant, the instantaneous power increases as the resonance is approached and decreases as the antiresonance is approached.

The fact that the transformation ratio of a planar piezoelectric transformer is inversely proportional to the squared frequency, explains the experimentally established decrease in this parameter at the upper frequencies of longitudinal vibration modes, which makes them ineffective, except for the first two resonances.

REFERENCES

1. D. Berlinkur, D. Kerran, and G. Jaffe, "Piezoceramic electric and piezomagnetic materials and their application in transducers," in: W. P. Mason (ed.), *Physical Acoustics, Principles and Methods*, Vol. 1, Part A, *Methods and Devices*, Academic Press, New York–London (1964).
2. I. A. Glozman, *Piezoceramics* [in Russian], Energiya, Moscow (1972).
3. A. A. Erofeev, G. A. Danov, and V. N. Frolov, *Piezoceramic Transformers and Their Application in Radio Electronics* [in Russian], Radio i Svyaz', Moscow (1988).
4. V. L. Karlash, "Transformation ratio and vibration modes of a planar Rosen-type piezoelectric transformer," *Elektrichestvo*, No. 1, 51–55 (2002).
5. V. L. Karlash, "Methods for determining the coupling coefficients for and energy loss in piezoceramic vibrators," *Akust. Visn.*, **15**, No. 4, 24–38 (2012).
6. V. V. Lavrinenko, *Piezoelectric Transformers* [in Russian], Energiya, Moscow (1975).
7. E. G. Smazhevskaya, R. F. Zhuchina, and N. A. Podol'ner, "Influence of the main parameters of a piezoceramic material on the characteristics of models of resonant piezoelectric transformers," in: *Radiators and Receivers of Ultrasonic Oscillations* [in Russian], Part II, LDNTP (1966), pp. 22–35.
8. N. A. Shul'ga and A. M. Bolkisev, *Vibrations of Piezoelectric Bodies* [in Russian], Naukova Dumka, Kyiv (1990).
9. M. O. Shul'ga and V. L. Karlash, *Resonant Electromechanical Vibrations of Piezoelectric Plates* [in Ukrainian], Naukova Dumka, Kyiv (2008).

10. M. O. Shul'ga and V. L. Karlash, "Amplitude–phase characteristics of radial vibrations of a thin piezoceramic disk at resonances," *Dop. NAN Ukrainy*, No. 9, 80–86 (2013).
11. Y. Fuda, K. Kumasaka, M. Katsumo, H. Sato, and Y. Ino, "Piezoelectric transformer for cold cathode fluorescent lamp inverter," *Jpn. J. Appl. Phys.*, **1**, 36, No. 5B, 3050–3052 (1997).
12. S. Hirose, N. Magami, and S. Takanashi, "Piezoelectric ceramic transformer using piezoelectric lateral effect on input and on output," *Jpn. J. Appl. Phys.*, **35**, 3038–3041 (1996).
13. R. Holland, "Representation of dielectric, elastic and piezoelectric losses by complex coefficients," *IEEE Trans. SU*, **SU-14**, 18–20 (1967).
14. "IRE Standards on Piezoelectric Crystals: Measurements of Piezoelectric Ceramics. 1961," *Proc. IRE*, **49**, 1161–1169 (1961).
15. V. L. Karlash, "Frequency properties of a planar piezoelectric transformer of longitudinal-transverse type," *Int. Appl. Mech.*, **36**, No. 8, 1103–1111 (2000).
16. V. L. Karlash, "The stress state of a rectangular piezoceramic plate with transverse–longitudinal polarization," *Int. Appl. Mech.*, **37**, No. 3, 386–392 (2001).
17. V. L. Karlash, "Electroelastic characteristics of a piezoelectric transformer plate," *Int. Appl. Mech.*, **39**, No. 7, 870–874 (2003).
18. V. L. Karlash, "Electroelastic vibrations and transformation ratio of a planar piezoceramic transformer," *J. Sound Vib.*, **277**, 353–367 (2004).
19. V. L. Karlash, "Longitudinal and lateral vibrations of a planar piezoceramic transformer," *Jpn. J. Appl. Phys.*, **44**, No. 4A, 1852–1856 (2005).
20. V. L. Karlash, "Longitudinal and lateral vibrations of a plate piezoceramic transformer," *U. J. Phys.*, **51**, No. 10, 985–991 (2006).
21. V. L. Karlash, "Admittance-frequency response of a thin piezoceramic half-disk," *Int. Appl. Mech.*, **45**, No. 10, 1120–1126 (2009).
22. V. L. Karlash, "Forced electromechanical vibrations of rectangular piezoceramic bars with sectionalized electrodes," *Int. Appl. Mech.*, **49**, No. 3, 360–368 (2013).
23. V. L. Karlash, "Energy losses in piezoceramic resonators and its influence on vibrations' characteristics," *Electronics and Communication*, **19**, No. 2 (79), 82–94 (2014).
24. V. L. Karlash, "Modeling of energy-loss piezoceramic resonators by electric equivalent networks with passive elements," *Mathematical Modelling and Computing*, **1**, No. 2, 163–177 (2014).
25. V. G. Karnaukhov, V. I. Kozlov, A. V. Zavgorodnii, and I. N. Umrykhin, "Forced resonant vibrations and self-heating of solids of revolution made of a viscoelastic piezoelectric material," *Int. App. Mech.*, **51**, No. 6, 614–622 (2015).
26. H. W. Katz (ed.), *Solid State Magnetic and Piezoelectric Devices*, Willey, New York (1959).
27. G. Liu, S. Zhang, W. Jiang, and W. Cao, "Losses in ferroelectric materials," *Mater. Sci. Eng.*, **89**, 1–48 (2015).
28. A. V. Mezheritsky, "Quality factor of piezoceramics," *Ferroelectrics*, **266**, 277–304 (2002).
29. A. V. Mezheritsky, "Elastic, dielectric and piezoelectric losses in piezoceramics; how it works all together," *IEEE Trans. UFFC*, **51**, No. 6, 695–797 (2004).
30. E. C. Munk, "The equivalent electrical circuit for radial modes of a piezoelectric ceramic disk with concentric electrodes," *Phillips Res. Rep.*, **20**, 170–189 (1965).
31. N. A. Shulga and V. L. Karlash, "Measuring the amplitudes and phase of vibrations of piezoceramic structural elements," *Int. App. Mech.*, **51**, No. 3, 350–359 (2015).
32. K. Uchino, J. H. Zheng, Y. H. Chen, et al., "Loss mechanisms and high power piezoelectrics," *J. Mat. Sci.*, **41**, 217–228 (2006).
33. K. Uchino, Yu. Zhuang, and S. O. Ural, "Loss determination methodology for a piezoelectric ceramic: new phenomenological theory and experimental proposals," *J. Adv. Dielectric.*, **1**, No. 1, 17–31 (2011).
34. S. O. Ural, S. Tuncdemir, Yu. Zhuang, and K. Uchino, "Development of a high power piezoelectric characterization system and its application for resonance/antiresonance mode characterization," *Jpn. J. Appl. Phys.*, **48**, 056509 (2009).
35. C. A. Rosen, US Patent 439 992 1954, June 29 (1954).
36. M. Yamamoto, Y. Sasaki, A. Ochi, et al., "Step-down piezoelectric transformer for AC-DC converters," *Jpn. J. Appl. Phys.*, **1.40**, No. 5B, 3637–3642 (2001).